

Purdue University Purdue e-Pubs

Earth, Atmospheric, and Planetary Sciences Faculty
Publications

Department of Earth and Atmospheric Sciences

1-1-2010

Observational evidence that agricultural intensification and land use change may be reducing the Indian summer monsoon rainfall

Dev Niyogi
Purdue University

Chandra Kishtawal
Space Applications Center, Indian Space Research Organization

Shivam Tripathi
Purdue University

Rao S. Govindaraju
Purdue University

Follow this and additional works at: <http://docs.lib.purdue.edu/easpubs>

Repository Citation

Niyogi, Dev; Kishtawal, Chandra; Tripathi, Shivam; and Govindaraju, Rao S., "Observational evidence that agricultural intensification and land use change may be reducing the Indian summer monsoon rainfall" (2010). *Earth, Atmospheric, and Planetary Sciences Faculty Publications*. Paper 132.
<http://dx.doi.org/10.1029/2008WR007082>

This document has been made available through Purdue e-Pubs, a service of the Purdue University Libraries. Please contact epubs@purdue.edu for additional information.



Observational evidence that agricultural intensification and land use change may be reducing the Indian summer monsoon rainfall

Dev Niyogi,¹ Chandra Kishtawal,² Shivam Tripathi,³ and Rao S. Govindaraju³

Received 9 April 2008; revised 6 August 2009; accepted 24 September 2009; published 30 March 2010.

[1] Using gridded daily rainfall observations, and monthly satellite land surface data sets, the connection between land use change and monsoonal rainfall climatology is analyzed. A combination of statistical analysis involving genetic algorithm (GA), empirical orthogonal function (EOF), and causal discovery algorithms (CDA) are used. Study objectives are (1) to identify regional trends in the observed precipitation data over the Indian summer monsoon region, (2) to investigate the relation between land use change/agriculture intensification and changes in rainfall, and (3) to explore whether land use change and agricultural intensification have *caused* change in the rainfall climatology. The satellite-based vegetation data set shows significant agricultural intensification over northern India. For the period just before start of the summer monsoon season (April and May), the normalized differential vegetation index (NDVI) shows an increase only over Peninsular India. The EOF- and GA-based analysis identified the strongest climatic signal for monsoon rainfall with an increasing trend over the east central regions of India and a decreasing trend in monsoon seasonal precipitation over north/northwest India. The areas of decreasing rainfall coincided with regions of agricultural intensive land use and are analyzed further. The correlation and the causal data analysis suggest that premonsoon (March–April) vegetation affects July month precipitation over peninsular India. In particular, a negative relationship exists between them. The results are more robust over peninsular and northern India indicating that an increase in NDVI has possibly weakened the early monsoon rainfall in this region. The results of this study suggest that land use change associated with agricultural intensification could be reducing the summer monsoon rainfall over certain regions of India.

Citation: Niyogi, D., C. Kishtawal, S. Tripathi, and R. S. Govindaraju (2010), Observational evidence that agricultural intensification and land use change may be reducing the Indian summer monsoon rainfall, *Water Resour. Res.*, 46, W03533, doi:10.1029/2008WR007082.

1. Introduction

[2] The Indian summer monsoon rainfall, defined here as the cumulative rainfall over continental India during June-to-September, has important socioeconomic implications over the Indian subcontinent [Fein and Stephens, 1987]. The initiation of the cross-equatorial flow off the Somalia coast of Africa during May in response to the heating over the South Asian continent marks the beginning of the Indian summer monsoon. There are indications that the intensive and large-scale human activities in Asia may have begun to impact the monsoon system [Intergovernmental Panel on Climate Change (IPCC), 2007; Goswami *et al.*, 2006; Kishtawal *et al.*, 2010]. Analysis of long-term rainfall data sets over the Indian subcontinent indicates epochal varia-

tions in the Indian summer monsoon rainfall [e.g., Mooley and Parthasarathy, 1984; Parthasarathy *et al.*, 1991; Sinha Ray and Srivastava, 2000]. Analyzing 100 years of surface rain gauge observations, Srivastava *et al.* [1992] showed that the mean monsoon seasonal rainfall has not changed significantly in the past century. However, recently Goswami *et al.* [2006] concluded that there are significant changes in the heavy ($>100 \text{ mm d}^{-1}$) and very heavy ($>150 \text{ mm d}^{-1}$) rainfall events over central India.

[3] Long-term trends in precipitation can result from either natural climate variability (e.g., decadal changes in circulation) or from anthropogenic factors, and accurate attribution is quite difficult [e.g., IPCC, 2007]. Some of the important anthropogenic activities that may affect regional monsoon rainfall climatology are the increase of greenhouse gases [Meehl and Washington, 1993], changes in radiative forcing due to aerosols and clouds [Ramanathan *et al.*, 2001, 2005], and changes in land surface physical properties due to land use changes such as urbanization and agricultural practices [Niyogi *et al.*, 2002a; Pielke *et al.*, 2002; Bonan, 2002]. These forcings can act in concert resulting in complex modification of the monsoon rainfall [Niyogi *et al.*, 2007].

¹Department of Agronomy and Department of Earth and Atmospheric Sciences, Purdue University, West Lafayette, Indiana, USA.

²Space Applications Center, Indian Space Research Organization, Ahmadabad, India.

³School of Civil Engineering, Purdue University, West Lafayette, Indiana, USA.

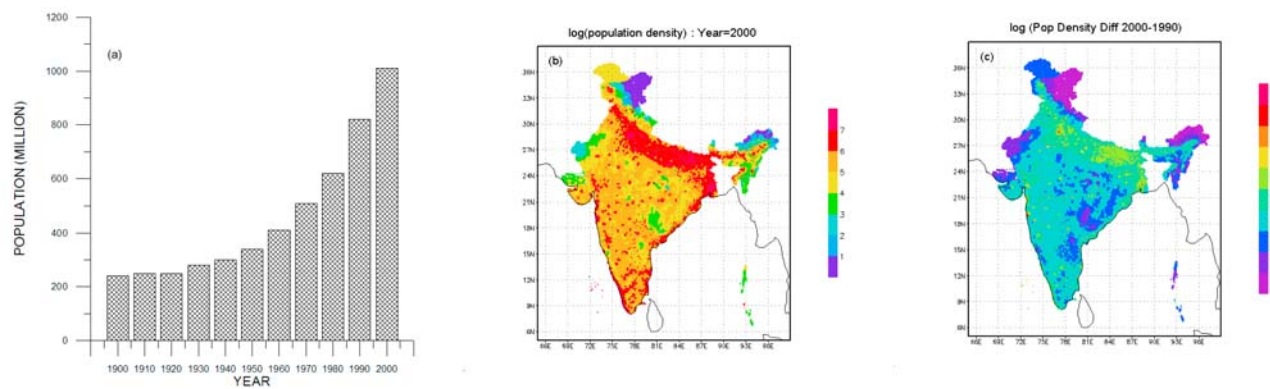


Figure 1. (a) Population of India from 1901 to 2001 based on official census reports. (b) Density of population (persons per square kilometer, values shown are natural log of actual numbers) over the Indian summer monsoon region for the year 2000. (c) Difference of the density of population (natural log of numbers shown) between the years 1990 and 2000.

[4] Majority of climate change studies over the Indian monsoon region have focused on the larger scale dynamics and relatively little attention has been paid to the effect of the regional land surface feedbacks on monsoon climate [Niyogi *et al.*, 2002a; Fu, 2003; Douglas *et al.*, 2006]. However, understanding the role of land surface feedback on the monsoon systems is important as the region shows dramatic land use land cover changes in response to the growing food and fiber requirements of a fast increasing population over the Asian monsoon region [Foley *et al.*, 2005].

[5] The land use change over India, in the recent decades, has primarily occurred because of urbanization [Kishtawal *et al.*, 2010] and intensive agriculture/irrigation practices [Douglas *et al.*, 2006, 2009]. Figure 1 shows the patterns of human settlement over the Indian summer monsoon region, on the basis of the official census reports (Office of the Registrar General and Census Commissioner of India) and population data set GPWv3 (Gridded Population of the World, version 3) produced by the Center for International Earth Science Information Network (CIESIN) of the Earth Institute at Columbia University. Figure 1a shows that the most intense population growth over India took place from 1960 onward. During the same period, India underwent significant transformations in farming practices in response to the “green revolution” (GR) [Roy *et al.*, 2007]. Some of the major highlights of GR were expansion of farming areas, double cropping over existing farmlands, and the development of a large irrigation system based on groundwater and network of canals [Goldman and Smith, 1995]. The areas most affected by GR were the parts of northwest India and the Gangetic plains, interestingly the region coinciding with the monsoon trough [Fein and Stephens, 1987]. Figures 1b and 1c show that not only does the area along the monsoon trough have the highest population density but this region also has the highest population growth rate in India.

[6] The impact of increasing population and resulting land use change on natural resources can be significant [O’Brien *et al.*, 2004; Foley *et al.*, 2005]. The impact of land use land cover change on rainfall has been reviewed by Pielke *et al.* [2007]. Feddema *et al.* [2005] used the Intergovernmental Panel on Climate Change scenarios and

simulated the effects of changes in land cover for different future climate scenarios using global climate modeling analysis. They found that the projected land cover transformation produces notable changes in the future climate and that agricultural expansion, in particular, could affect monsoon circulation. Douglas *et al.* [2006, 2009] showed that agricultural irrigation can impact regional evapotranspiration, surface radiative balance, and hypothesized through a modeling case study that these changes in surface characteristics can affect mesoscale convection and rainfall over the Indian monsoon region. Roy *et al.* [2007] analyzed a century long monthly temperature data set over India and showed that the pre- and post-agricultural GR temperature regimes have different characteristics. In particular, Roy *et al.* concluded that the lack of significant warming over India in the post-GR could be in part due to agricultural intensification and irrigation. Lee *et al.* [2008] recently suggested that the variation of the early summer monsoon rainfall over India may be partially a result of irrigation/increased agriculture. Yet an observational analysis assessing the causal relationship between agricultural intensification/land use land cover change and rainfall changes over the Indian monsoon region is still lacking.

[7] With the availability of high-resolution gridded data of daily surface rainfall observations over India [Rajeevan *et al.*, 2006], and the monthly satellite land cover data sets [Tucker *et al.*, 2005; Basist *et al.*, 1998], it may be possible to identify the effects of land use changes on the regional Indian monsoon climate. Accordingly, the aims of this work are (1) to identify regional trends in the observed precipitation data over the Indian summer monsoon region, (2) to investigate the relation between land use change/agriculture intensification and change in rainfall, and (3) to explore whether land use change/agricultural intensification has caused change in rainfall.

[8] The Indian summer monsoon is briefly summarized in the following section. The data used in the study are described in section 3. An approach involving empirical orthogonal function (EOF) and genetic algorithm (GA) is adopted to explore dominant climatic trends from the available long-term rainfall observation and is discussed in section 4. Methods for detecting causal relationships between observed precipitation trends and regional land

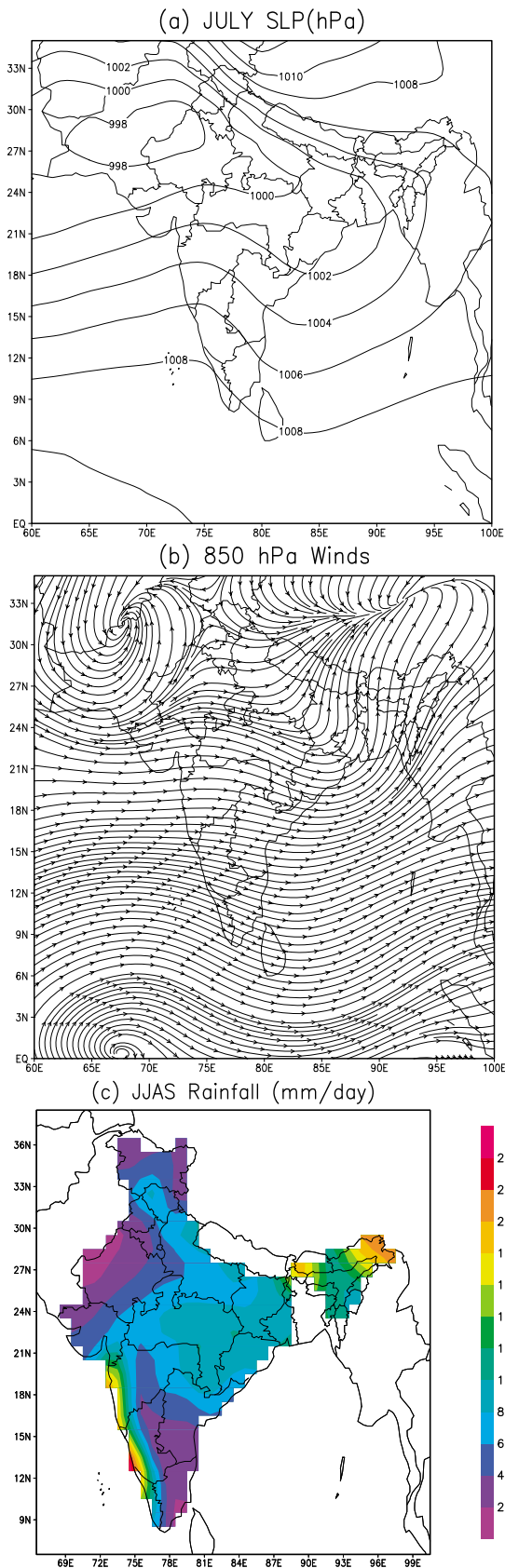


Figure 2. (a) Mean sea level pressure (MSLP, hPa) during July, (b) 850 hPa circulation, and (c) average daily rainfall during monsoon season. MSLP and 850 hPa winds are based on NCEP/NCAR reanalysis while rainfall is from IMD data. Averaging period is 1951–2003.

use changes are discussed in section 5. Results of the analysis are presented in section 6. Study conclusions are provided in section 7.

2. A Brief Overview of Indian Summer Monsoon

[9] The Indian summer monsoon season typically begins in late May to early June. By late May, positive rainfall anomalies are limited mainly to the western part of Indochina peninsula, the Indian Ocean and the western Pacific at around 30°N. By early June, positive rainfall anomalies begin to develop west of the Indochina peninsula, the Bay of Bengal and the Indian peninsula, marking the onset of the Indian monsoon. The seasonal cycle of the precipitation anomaly averaged over India at this time shows a sharp increase, and the first peak typically appears during 10–14 June. This transition to the Indian monsoon is characterized by the development of the low level cyclonic circulation anomaly, the upper level anticyclone, and convective activity in south and southeast Asia. The location of these positive precipitation anomalies is intimately related to the development and the northward progression of the negative pressure anomaly over India. The migration of the pressure anomaly toward northwest Indian subcontinent during July appears to determine the pathway of moisture during the mature stage of the monsoon (Figures 2a and 2b). Specifically, a strong pressure gradient along the monsoon trough extending from southeast in the Bay of Bengal to northwest in Pakistan produces a strong southeasterly wind, which serves as a conduit for moisture transport from the Indian Ocean to most of the northwest and north central regions of Indian peninsula. The typical pressure anomaly configuration of the Indian summer monsoon (high pressure over ocean and low pressure over land) also supports the genesis and development of a number of low-pressure transient systems that cause significant variability in the monsoonal rainfall. After mid-August, the Indian summer monsoon undergoes a gradual decaying phase.

[10] The Indian summer monsoon system is also characterized by strong intraseasonal oscillations (ISO) with active (wet) and break (dry) cycles [Yasunari, 1979]. The active-break cycle of the monsoon system is a manifestation of repeated northward propagation of the tropical convergence zone (TCZ) from the equatorial position to the continental position [Sikka and Gadgil, 1980] and results from superposition of a 10–20 day and a 30–60 day oscillations [Goswami, 2004]. Monsoon seasons with higher than average rainfall generally show a smaller period of active-break cycle while during the drought years this period seems to extend for a longer time [Kishtawal et al., 1991]. The active-break cycle is also associated with the alteration of large-scale circulation features. During a typical active phase, the low level westerlies strengthen over the Arabian Sea, which is replaced by the easterly anomalies during a break phase [Webster et al., 1998]. The northward propagating 30–60 day ISO-mode has a large spatial scale encompassing south Asia and east Asia and west north Pacific ocean, while the westward propagating 10–20 day oscillation has a smaller zonal scale and is regional in character [Goswami, 2004]. The amplitude of the dominant mode of ISO is so significant (with respect to seasonal mean precipitation) that the frequency of occurrence of these oscillations are capable of influencing the seasonal rainfall

and thus can contribute to the inter annual variability of monsoon [Goswami, 2004].

[11] Embedded within these large-scale forcings is the modulation of the mesoscale convection due to surface and boundary layer processes and may cause significant variability in the monsoon rainfall [Niyogi et al., 2002a; Pielke et al., 2003]. While the feedback of the synoptic and large-scale processes on monsoon rainfall is relatively well understood, the effect of land surface processes and land use land cover changes, such as being studied in this paper, are only recently evolving [e.g., Niyogi et al., 2002a; Douglas et al., 2006; Lee et al., 2008].

3. Data

3.1. Rainfall Data

[12] Daily gridded rainfall data at 1° grid spacing from India Meteorological Department (IMD) [Rajeevan et al., 2006] were used. This data set is based on 1803 stations over India with a minimum 90% data availability during the period 1951–2003. Using these station data, the grid point analysis of rainfall was prepared by using Shepard's directional interpolation method [Shepard, 1968] over the Indian subcontinent ($6.5\text{--}37.5^\circ\text{N}$, $66.5\text{--}101.5^\circ\text{E}$). Standard quality controls were performed before carrying out the interpolation analysis. Because of averaging, the gridded rainfall data are smoother compared to individual station data. Average of daily rainfall for 122 day long monsoon season (June-to-September) was carried out at each 1° grid point and was used for the trend analysis. Figure 2c shows the average daily rainfall during monsoon season based on the IMD rainfall data set. To overcome the effect of spatial inhomogeneity of rainfall on the calculation of regional trends, we first normalized the time series of seasonal rainfall with respect to its 53 year average (1951–2003) at each grid cell. To determine the causal relationship between rainfall and agriculture, we used monthly area weighted rainfall data of 29 meteorological subdivisions in India [Parthasarathy et al., 1994], which extend from January 1948 to December 2002. These data are prepared by Indian Institute of Tropical Meteorology, Pune (<http://www.tropmet.res.in>), using a subset of IMD's surface rainfall observation network that was used for producing gridded rainfall data.

3.2. Remote Sensing Based Land Cover Data

[13] We used monthly mean normalized differential vegetation index (NDVI) data based on the observations from Advanced Very High Resolution Radiometer (AVHRR) on board NOAA series of satellites. This data set is prepared by Global Land Cover Facility, University of Maryland [Tucker et al., 2005], and is archived by International Research Institute for Climate and Society (IRI), Columbia University, New York at <http://ingrid.ldgo.columbia.edu/SOURCES/UMD/GLCF/GIMMS/NDVIg/>.

[14] The data span from July 1981 to December 2003 at 0.073° spatial resolution. While the data have been corrected for view geometry, volcanic aerosols, and other effects not related to vegetation change, they have some known uncertainties over the Indian monsoon region [e.g., Jeyaseelan et al., 2007].

[15] Special Sensor Microwave/Imager (SSM/I) based weekly surface wetness index (BWI) derived by Basist et al. [1998] were also used. This index is based on the passive

microwave radiometer data at four frequencies (19.35, 22.235, 37.0, and 85.5 GHz) and dual-polarization (except at 22.235 GHz). The weekly compositing scheme is used to generate global gridded product from swath data at regular temporal period and to avoid the atmospheric influence in assessment of land surface wetness condition. The weekly composite BWI data from National Climatic Data Centre (NOAA/NESDIS) at 0.3° spatial resolution were used.

4. Methodology

4.1. Determining Climatic Patterns Using EOF and GA

[16] To determine the strong and coherent regional climatic signals in the rainfall observations, the following question were posed: What is the largest region over Indian summer monsoon domain for which the long-term rainfall trends are largest irrespective of the sign of the trend? Identification of such regions is important for studying the land use land cover change impacts, as regions that are scattered may not form a detectable regional response on mesoscale convection and rainfall. We employed an EOF analysis [Peixoto and Oort, 1992] and a GA technique [Mitchell, 1998].

[17] EOF is a statistical tool that compresses geophysical data fields in space and time. The technique allows one to explain the variance-covariance of the data through a few modes of variability. This method is effective in identifying leading modes in temporally varying spatial patterns (eigenvectors) and their corresponding principal components (time series) and ranking them according to the percentage of total variance explained in the data of interest [Peixoto and Oort, 1992]. In the present analysis, the mean rainfall for July month was subjected to the EOF analysis.

[18] Genetic algorithms are powerful general-purpose tools which mimic the process of natural selection by setting up a population of artificial "organisms" (possible solutions) and allowing them to evolve based on selection pressures defined by the objective of the problem. In the present context, the objective is to discover a coherent region over Indian monsoon domain that shows the strongest climatic signal [e.g., Kishtawal et al., 2003]. Thus, the population of "organisms" consists of a number of such possible patterns and the "selection pressure" is the magnitude of the long-term trend of area-averaged rainfall for such patterns which we want to maximize. A flowchart of the GA-process adopted in this study is given in Figure 3.

[19] The GA procedure was initiated with a large number (400 in this case) of random yet coherent patterns formed by a cluster of $1^\circ \times 1^\circ$ grid cells. Each pattern in turn was scored according to the long-term trend of summer-monsoon rainfall averaged over that pattern. Individual patterns with strongest trends would get the highest score. The variation inherent in the initially random population of patterns would ensure that some patterns scored better than others. These scores would then become the fitness measures of the individual patterns and subsequently dictate the proportional makeup of the next generation. The most fit patterns would be disproportionately represented in the next generation, while those poorer scorers would be underrepresented or drop out of the population altogether.

[20] A process where features of the individual patterns are swapped between pairs ranked in order of fitness scores

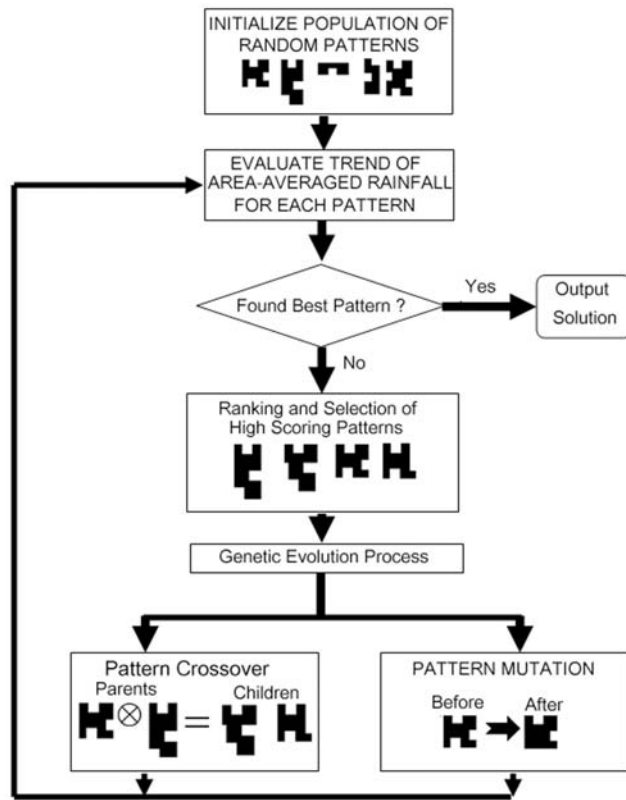


Figure 3. A flowchart for GA process used in the present study.

is then typically used. This produces a composite pattern from each pair and is the artificial version of genetic reproduction. Each pair patterns can be considered the parents of each composite child. This is an effective method of mixing pattern features to produce composite children some of which will score better than their parents. Intermittently, small random variations in selected patterns are also typically used during reproduction; this adds noise to the process and by doing so helps increase the efficiency of convergence on an optimal pattern. This is the artificial version of genetic mutation. The next generation of patterns is then scored based on the long-term trends of pattern-averaged rainfall time series. After a large number of generations, the test-and-reproduce cycle is expected to move the overall population of patterns in the direction of the optimal pattern as only the highest scoring patterns in each generation will survive in to the next. Eventually, a pattern is expected that gains the best score and this pattern of grids can be considered as an area that shows largest climatic signal, e.g., trend.

4.2. Exploring Causal Relationship Between Rainfall and Regional Land Use Change

[21] A speculative, but as yet unsubstantiated, relation between land use change over India and changes in Indian summer monsoon rainfall was studied using causality arguments on observations. Correlation analysis is arguably the most popular statistical tool for deciphering relations between hydroclimatic variables from observed data [Krishnamurti et al., 1999]. Although correlation analysis

is a useful tool, it is not suited for this study because our goal is not merely to investigate the relation between agricultural land use change and changes in rainfall but also to explore whether land use change such as agricultural intensification has *caused* change in rainfall. Correlation analysis cannot identify such causal relationships.

[22] Causality and detection of causal relationships has traditionally been a subject of metaphysics [Hume, 1999]. However, building on the research over past two decades, it is now possible to define causality mathematically using the concepts of probability and graph theory. Tools have been developed to discover cause-effect relationships in nonexperimental data under some reasonable assumptions [e.g., Pearl, 2000; Spirtes et al., 1993]. This study builds on these recent advances to explore causal relationships between increased agricultural intensification/irrigation over India and changes in monsoon rainfall. Two causality detection algorithms that are based on different approaches and have different sets of assumptions were selected.

[23] The causal discovery algorithms used in this study fall under the category of functional causal models called *structural equations*. In these models, causal relationships among variables are expressed in the form of deterministic functional equations. In linear structural equation models, each variable is expressed as a linear sum of its causal variables plus an exogenous error term. Given a set of observed variables x_i , $i \in \{1, 2, \dots, m\}$, the structural equations are given by

$$\alpha_{ik}x_i = \sum_{k \neq i} \alpha_{ik}x_k + \varepsilon_i, \quad i = 1, 2, \dots, m, \quad (1)$$

where α_{ik} are linear coefficients and ε_i are error or perturbation terms. The error terms are often assumed to be independent, i.e., $p(\varepsilon_1, \varepsilon_2, \dots, \varepsilon_m) = \prod_{i=1}^m p_i(\varepsilon_i)$. A set of the equations of the form given by equation (1) in which each equation represents an autonomous mechanism is called a structural model.

[24] Structural equation model is traditionally used as a tool to test hypothesis of causal relationships in data. However, recently algorithms have been proposed that allow searching of possible causal relationships in nonexperimental data. In this study, the following two algorithms were employed:

[25] (1) *Cyclic causal discovery* (CCD) algorithm: CCD algorithm [Richardson, 1996] is designed to investigate existence or nonexistence of causal relationships among variables in nonexperimental data. The algorithm assumes that the true causal structure can be cyclic and that there is no common cause between any two variables (confounders) in the data set. Further, it assumes that the disturbance terms (ε_i in equation (1)) are normally distributed, independent, and have nonzero variance. The algorithm ensures discovery of correct causal model under a large sample limit. The algorithm used in this work is available under Tetrad project from Carnegie Mellon University (<http://www.phil.cmu.edu/projects/tetrad>).

[26] (2) *Linear non-Gaussian acyclic model* (LiNGAM): The LiNGAM algorithm [Shimizu et al., 2006] assumes that the true causal relationship in the data is linear, acyclic, and there are no unobserved confounders. It further assumes that error terms in equation (1) are independent and have non-

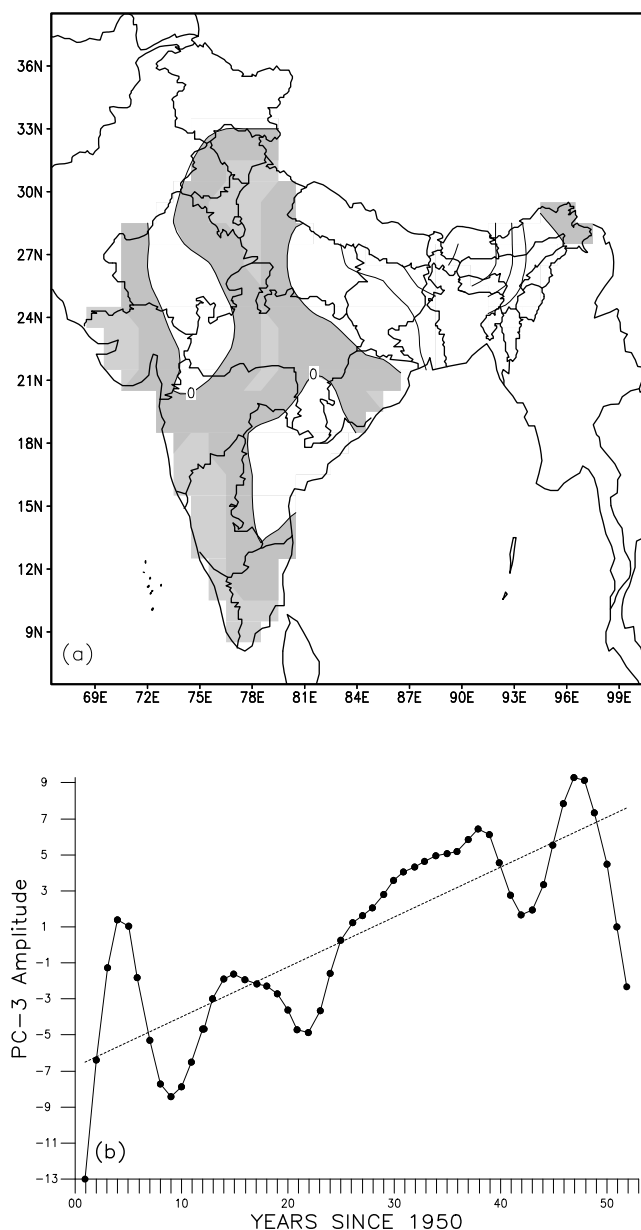


Figure 4. (a) Third leading mode (EOF-3) for July rainfall over India (regions with negative values are shaded) and (b) low-pass filtered time series of the amplitude of EOF-3 for July mean rainfall.

Gaussian distribution with nonzero variance. LiNGAM uses independent component analysis, a multivariate statistical analysis to discover causal structure in the data. The assumption of non-Gaussianity allows algorithm to go beyond second-order statistics (i.e., the covariance matrix) and discern full causal structure in the data [Shimizu *et al.*, 2006]. A Matlab implementation of the algorithm was obtained from the developers (at <http://www.cs.helsinki.fi/group/neuroinf/lingam/>).

[27] The first step toward understanding the impact of agricultural intensification on Indian summer monsoon rainfall was to assess the increase in NDVI values over India during the study period. Trends in the NDVI values were estimated using regression analysis and nonparametric Mann-Kendall trend test.

[28] Correlation analysis is recommended as a preliminary step for detecting presence of causal relationships [Spirtes *et al.*, 1993]. Existence of correlation between variables is a necessary, but not sufficient condition for causality. In accordance with these recommendations, correlation analysis between NDVI and rainfall over meteorological subdivisions of India was performed before applying the causal discovery algorithms.

5. Results

5.1. EOF and GA Analysis

[29] For the period of analysis (1951–2003), the mean seasonal monsoon rainfall over India was 861 mm with a standard deviation (SD) of 95.6 mm. There were only 2 years (1972 and 1987) during which the seasonal rainfall deviated from the mean rainfall by 2 SD. There were 6 years (1961, 1965, 1972, 1979, 1987, and 2002) for which the deviation was larger than 1.5 SD. In order to examine the trends when extreme years are removed, new time series were constructed for each region by replacing rainfalls for the abnormal years by mean values for the respective regions. Even after removing extreme years from the analysis, the nature of trends did not change, although the magnitude of the trends got reduced (to +0.044 from +0.054 for east central India, and to -0.031 from -0.042 for northwest India, and a near zero trend when considering entire India). This further indicates that the trends shown have their origin in some regional process.

[30] Consequently, for the EOF analysis, the first two leading modes (EOF-1 and EOF-2) explained 21% and 16% of the total variance, respectively. These two modes represent the spatial structure of mean-monsoon climatology and its intra- and interannual variability, and do not show a noticeable long-term trend. However, the third leading mode, EOF-3, which explains about 10% of the variance shows a significant trend through the length of the rainfall data (Figures 4a and 4b). The spatial distribution of the eigenvector covers regions of north/northwest India and some parts of peninsular India (Figure 4a). This structure indicates that the long-term variations (trends) in summer rainfall in north/northwest and west-peninsular India are in phase with each other but are out of phase with the variation in eastern part of India (particularly east India and east-peninsular India). The corresponding time series (Figure 4b) shows a multidecadal secular trend (more prominently after the 1960s agricultural GR). This trend is statistically significant at the 99% confidence level. A strong year-to-year variation is also observed in EOF-3. Combining the spatial distribution of the eigenvector and the associated time series of the EOF-3 mode, it appears that there has been a continuous increase in the summer rainfall over the east India and a decrease over north/northwest India during the past five decades.

[31] Although EOF is a powerful technique to determine temporal covariance of spatial patterns, it is difficult to ensure that the EOF technique picks up the regions of strong trends, which is one of the main objectives of the present study. By design, EOF determines mutually uncorrelated (orthogonal) spatial patterns, whose temporal variability may or may not be related to trend. Therefore, to address the issue of determining the regional spatial patterns with

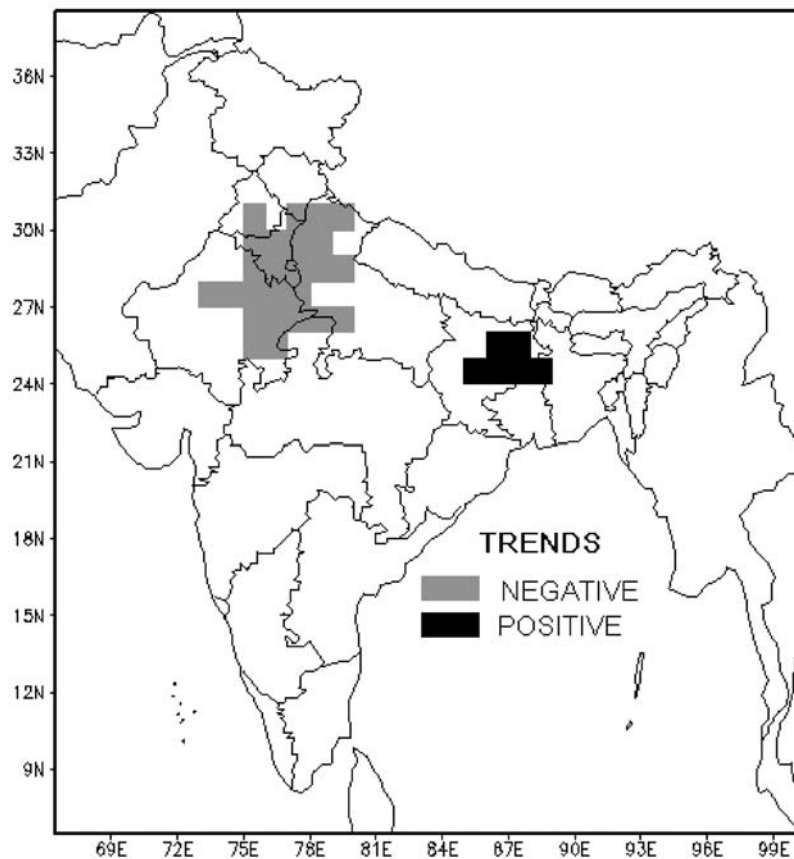


Figure 5. Regions of strong positive and negative trends in monsoon seasonal rainfall determined by GA approach.

strong temporal trends, we employed a GA-based approach, in which the spatial patterns can be determined using a user-defined constraint such as the strength of the long-term trend.

[32] In the GA analysis, we excluded the domain above 33°N due to poor station density and large topographical variations leading to higher uncertainty while searching for regions with strongest trends. Figure 5 shows the areas determined by GA for which the area-averaged values of normalized rainfall (R_N) show the strongest positive and negative trends during 1951–2003. The strongest climatic signal that appears from the available rainfall data indicates an increasing trend over the east central regions such as West Bengal/Bihar and a decreasing trend in monsoon seasonal precipitation over northwest India. Interestingly, both of these regions of strong yet opposite trends lie along the monsoon trough, an axis characterized by strong southeast-to-northwest pressure gradient during the monsoon season (Figure 2b). This result is consistent with the changes in the surface heat fluxes patterns found by Douglas *et al.* [2006].

[33] The large region with a negative trend in precipitation, about $0.25 \times 10^6 \text{ km}^2$ in size ($\sim 8\%$ of the area of India), includes portions of three states: Punjab, Haryana, and western Uttar Pradesh. Two of these states (Punjab and Haryana) had statistically significant decrease in the surface sensible heat flux in the study of Douglas *et al.* [2006, Table 3b]. Interestingly, the region with negative rainfall trend also figures prominently in the economic map of India

due to its high agricultural yield. The agricultural practices in this region rely more on the improvised irrigation system fed by groundwater and canals from major rivers, and less on the seasonal rainfall [cf. O'Brien *et al.*, 2004]. Recall that in the post-GR, the agricultural practices in NW and NC India went through a drastic change [Roy *et al.*, 2007]. Figure 6 shows that over the northwest region of India, the average seasonal rainfall has decreased by 35%–40% with respect to its long-term average, during the past 53 years while over a smaller region over West-Bengal/Bihar, it has increased by about 40%–45%. Interestingly, seasonal mean rainfall averaged over the whole of India does not show a significant trend during the same period (Figure 6a). This indicates that despite the stability of Indian summer monsoon rainfall, strong regional variations and trends exist within the monsoon system, which may be indicative of the local processes affecting precipitation characteristics [Niyogi *et al.*, 2007]. The reduction in the rainfall over the intensive agricultural region is analyzed further in this paper. The increased rainfall over the smaller region of West Bengal/Bihar is not analyzed in this study but could be a result of urbanization [Kishtawal *et al.*, 2010], and enhanced thunderstorm and monsoon depression activity [Houze *et al.*, 2007; Chang *et al.*, 2009; Medina *et al.*, 2010].

[34] Figure 7 shows the spatial distribution of the SSM/I based soil wetness (BWI) averaged for month of May during 4 years. Figure 7 clearly indicates that there is a significant premonsoon soil moisture hot spot over the north/northwest India and adjoining parts of Pakistan. A

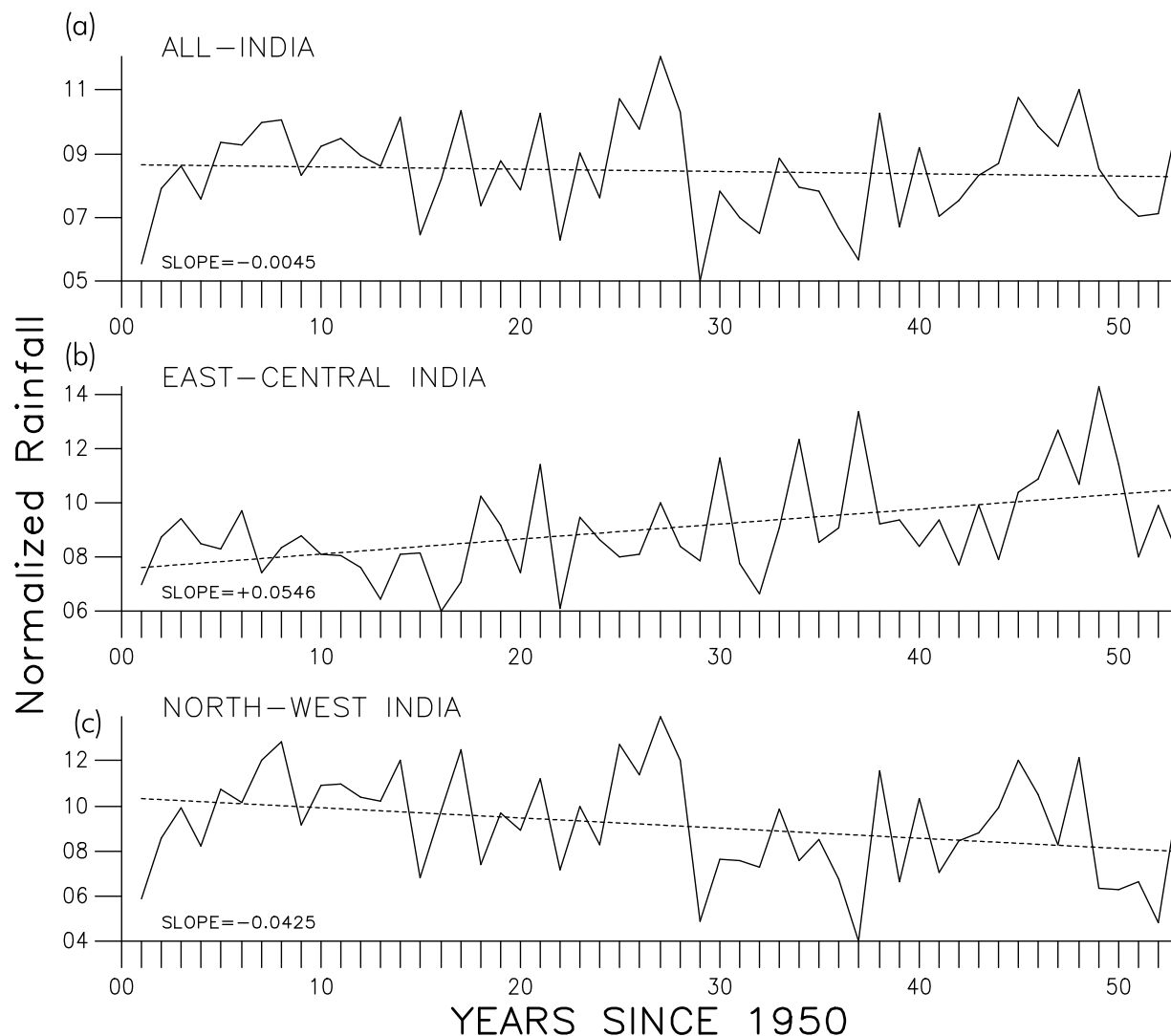


Figure 6. Linear trends in the rainfall averaged over (a) all-India, (b) east central India (dark shaded region in Figure 4), and (c) northwest India (light shaded region in Figure 4). Rainfall values were normalized with respect to their long-term mean before averaging to make the comparison simple.

trend analysis of 5 week average (covering the month of May) soil-wetness over a $5^{\circ} \times 5^{\circ}$ region ($74\text{--}79^{\circ}\text{E}$; $29\text{--}34^{\circ}\text{N}$) over the northwest India indicates a 300% increase in premonsoon soil wetness between the year 1988 and 2002 (Figure 8).

[35] The increased soil moisture could be a combined effect of agricultural intensification [Joshi and Tyagi, 1991], irrigation [Douglas *et al.*, 2009], and to some degree regional thunderstorm activity [Houze *et al.*, 2007]. Since a threefold to fivefold increase has occurred in the values of area-averaged soil moisture between 1988 and 2002, the thunderstorm activity cannot be expected to increase by that factor without some dominant regional or large-scale forcing. We compiled agricultural statistics for Punjab and Haryana (two dominant agricultural states in NW India). Between 1971 and 1991, the number of tube-wells in Haryana increased from 33.9 to 143.6 per thousand hectares, which is consistent with the rate of increase in soil moisture shown in our analysis. Between 1960 and 1990, the area devoted to wheat cultivation increased by 150%

while the area used for water-intensive paddy cultivation increased 3 times. A significant portion of this paddy cultivation occurs during the premonsoon season and is mostly irrigated using the groundwater. In a recent study, using multitemporal remote sensing data, Singh *et al.* [2006] showed that the average rice crop cycle (cultivation to harvest) has advanced by about 4 weeks over the northwestern Indian states of Punjab and Haryana between 1981 and 2000. Thus, the change in the regional vegetation phenology is a likely result of shift from monsoon-based irrigation to groundwater irrigation during the replanting stage of the rice crop, resulting in a significant regional-scale anthropogenic modification of soil moisture and soil hydrology during premonsoon phase (late-May to early June).

[36] This increase in the soil moisture due to irrigation and agricultural intensification during the premonsoon phase is a dominant regional forcing that can alter the regional circulation and precipitation patterns and is analyzed in the following section.

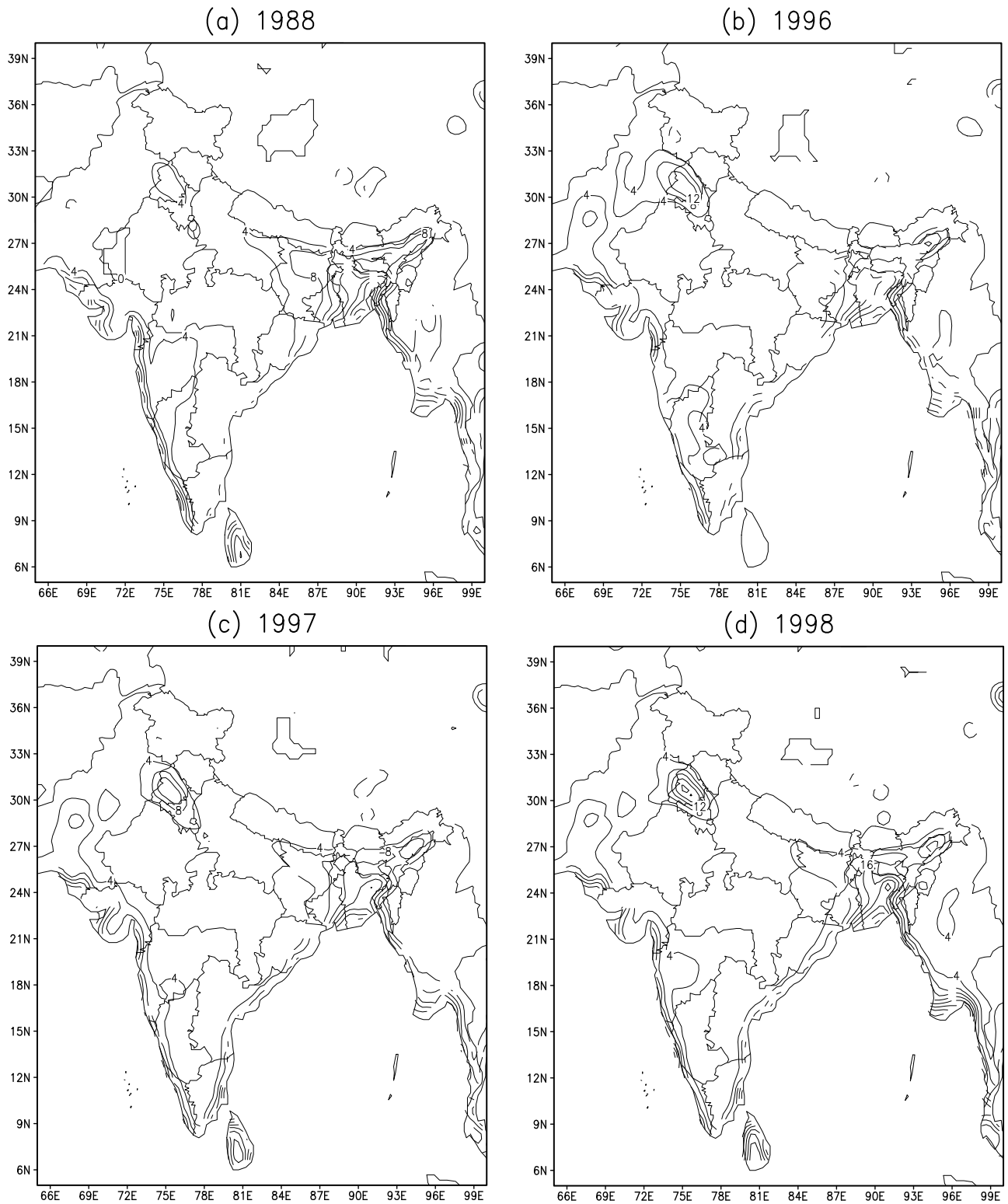


Figure 7. SSM/I-derived soil wetness index, BWI, for premonsoon phase (average for May) for four different years.

5.2. Causal Analysis

[37] The regional-scale changes in vegetation and soil wetness can significantly modify the radiative balance over a large area, resulting in a net cooling of the surface [Roy *et al.*, 2007], as well as alter the mesoscale convection [Douglas

et al., 2009]. This in turn can affect the intensity of seasonal negative pressure anomaly over the northwest Indian peninsula and result in weaker pressure gradients along the northwest/southeast axis [cf. Lee *et al.*, 2008]. The seasonal low-pressure anomaly over the northwest Indian subcontinent determines the pathway of moisture during the mature

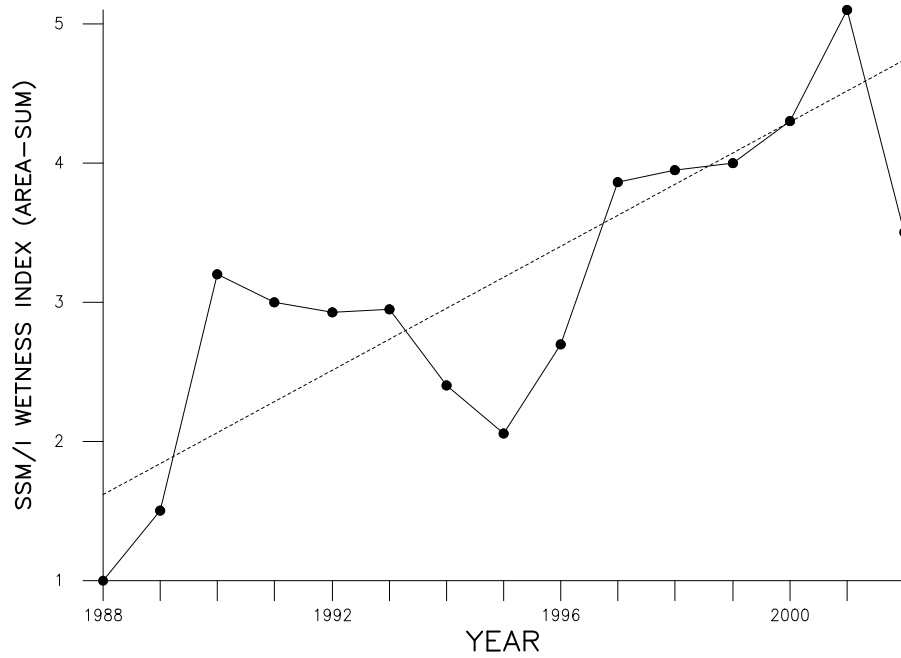


Figure 8. Long-term variation of $5^{\circ} \times 5^{\circ}$ averaged soil wetness index for the month of May over the north/northwest India.

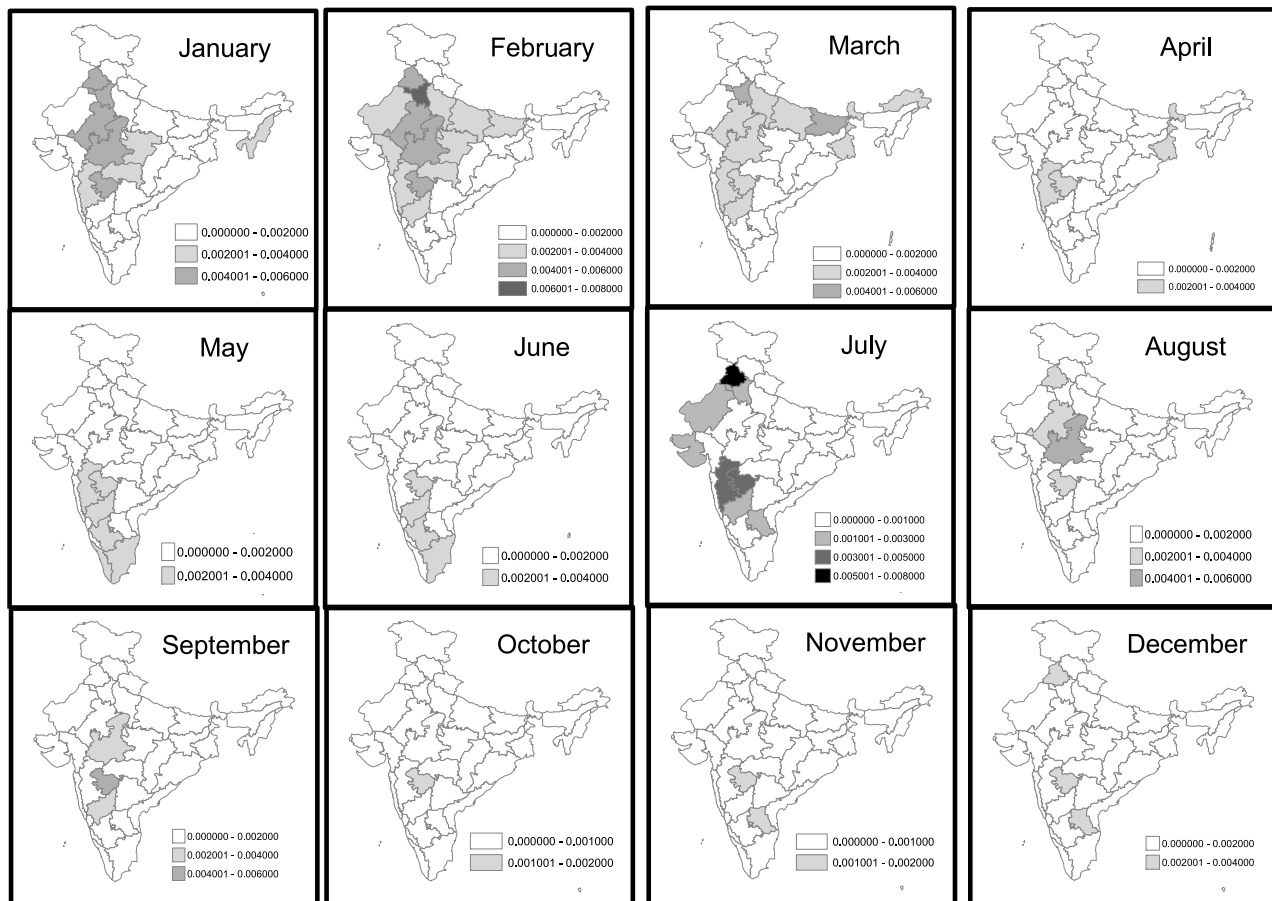


Figure 9. Results from the trend analysis of NDVI time series for different subdivisions. Shaded regions have trend significant at 10% level.

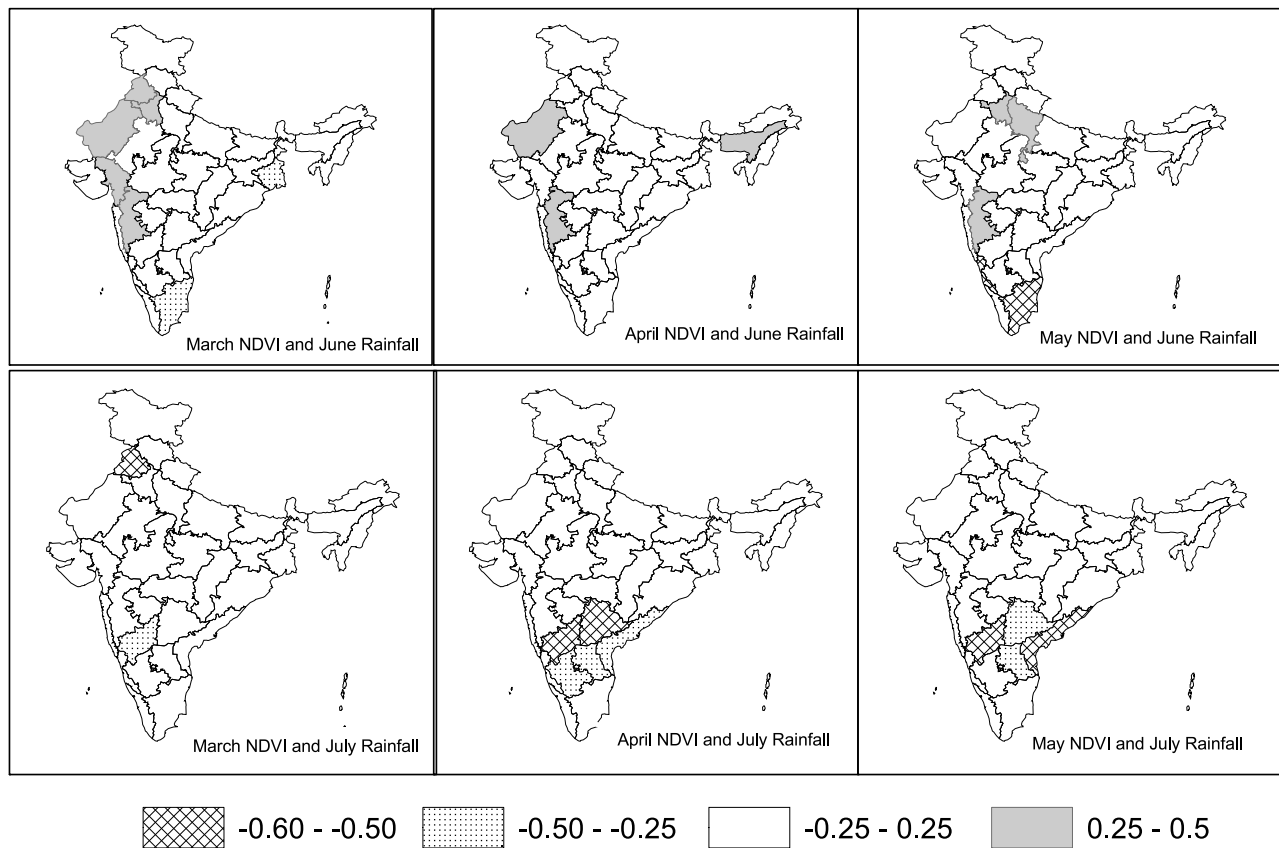


Figure 10. Correlation between NDVI values in premonsoon months (March–April–May) and early summer monsoon rainfall (June–July) over different subdivisions. Subdivisions with correlation significant at 10% level are shaded.

stage of the monsoon (Figures 2a and 2b), and this pressure anomaly is arguably the dominant forcing that determines the occurrence and intensity of monsoon rainfall over the north/northwest India. This low-pressure anomaly is maintained by the seasonal heating of northwest Indian subcontinent. One consequence of agricultural intensification thus can be the weakening of the forces that are crucial for advancing the Indian summer monsoon up to its north and northwest limits.

[38] To investigate this relation between the changes in rainfall and land use changes, we explored the causal relationships using a composite analysis of rainfall and NDVI. The long-term spatial and temporally averaged monthly changes in NDVI during the study period (1981–2003) are illustrated in Figure 9. Figure 9 shows slopes of the linear regression line fitted to NDVI time series for different meteorological subdivisions.

[39] In Figure 9, the NDVI for the period January to March shows the largest positive trend. These months also coincide with the period of intense irrigation during the winter rabi season (November to May). The increase is confined over the northern India region that includes the states of Haryana, Punjab, west Uttar Pradesh, east Rajasthan, and west Madhya Pradesh where rabi season crops are most important. This also includes the region where the GA approach identified a significant rainfall trend. Thus, this increase in NDVI values can be partly attributed to increase in agricultural land use over those areas.

[40] For the April, May, and June months, the NDVI values show an increase mainly over Peninsular India with no appreciable increase in other parts of the country. In May, just before the monsoon onset, the NDVI changes are confined primarily to Peninsular India. For brevity, only the results obtained from linear trend analysis are presented. Qualitatively similar results were obtained from nonparametric Mann–Kendall trend test.

[41] The result of correlation analysis for premonsoon months NDVI and early monsoon rainfall are shown in Figure 10. Negative correlation between July rainfall and March–April–May NDVI over subdivisions in Peninsular India is evident from Figure 10. A similar relation was recently reported by *Lee et al.* [2008] using the 2.5° resolution Global Precipitation Climatology Project ver.2 [Adler et al., 2003] rainfall data and NDVI data. These recent results along with results presented in Figure 9 suggest that the increased NDVI values over Peninsular India may have weakened the early monsoon rainfall in that region. However, other meteorological subdivisions in India do not show any evidence of change in early monsoon rainfall due to change in NDVI. Also, the correlations between NDVI values prior to March and monsoon rainfall were not significant.

[42] Figure 11 shows the simultaneous correlations between NDVI values and rainfall during monsoon months. For the month of July, rainfall and NDVI values are negatively correlated over many meteorological subdivi-

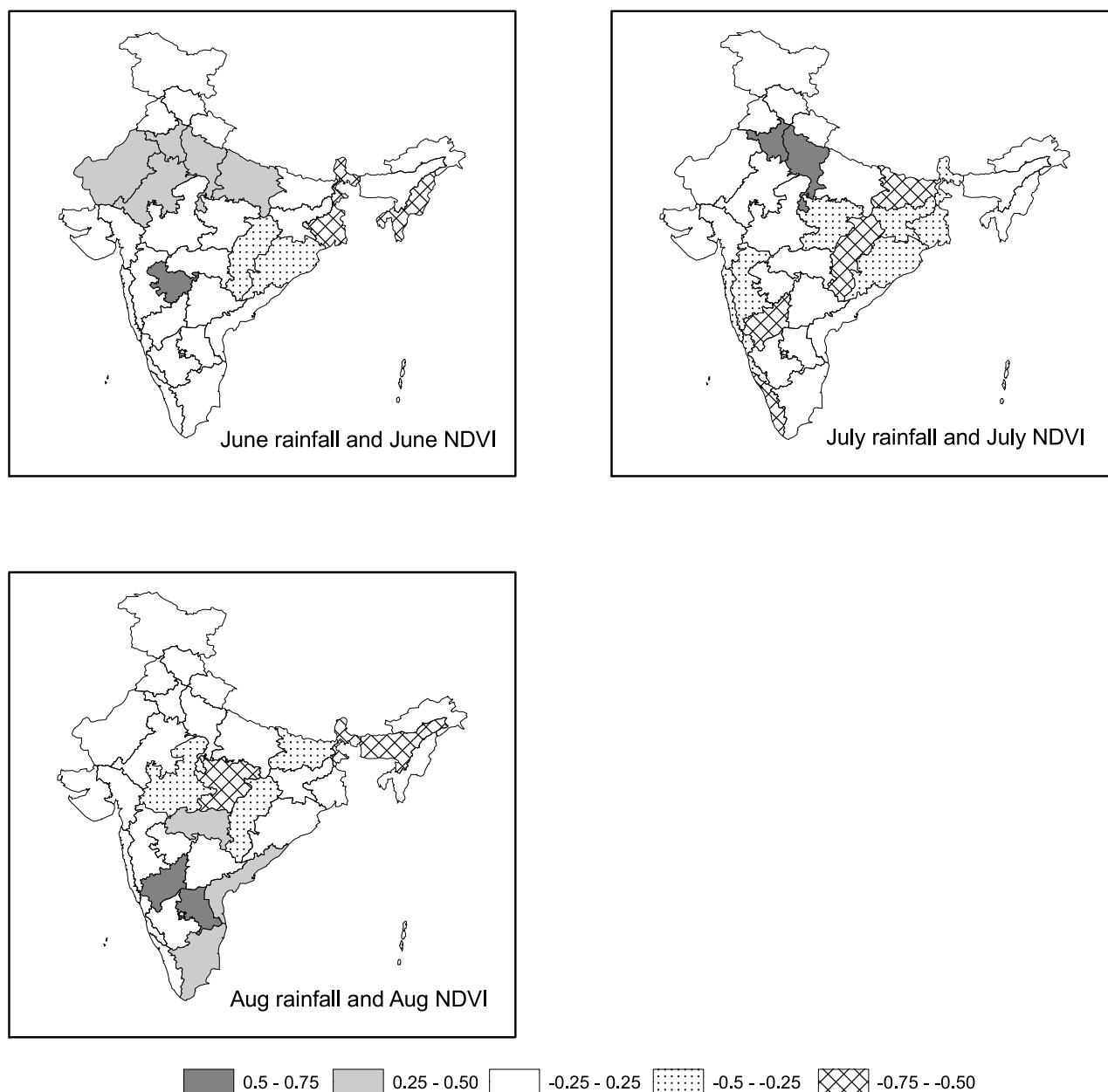


Figure 11. Simultaneous correlation between NDVI values and rainfall during monsoon months (June–July–August). Subdivisions with correlation significant at 10% level are shaded.

sions. This suggests two scenarios: either the higher NDVI weakens the monsoon or, the Indian summer monsoon gains strength because of low NDVI values. The correlation between current month NDVI and previous month rainfall values is analyzed next (Figure 12). As expected, the correlations are positive over most of the climate subdivisions highlighting the logical conclusion that the higher rainfall in present month will lead to more vegetation in the subsequent month.

[43] Correlation analysis is indeed not sufficient to explain the causality between NDVI and monsoon rainfall changes. Accordingly, Figure 13 shows the results of causal discovery algorithm applied to test the cause-effect relationship between premonsoon NDVI and early monsoon rainfall suggested by correlation analysis (Figure 10). The results correspond to climate subdivisions approximately between

12°N and 18°N/southern India (including coastal Andhra Pradesh, southern interior Karnataka, and northern interior Karnataka) that yielded significant correlations. In Figure 13, the arrowhead at the end of an edge indicates direction of causal relationship (e.g., r_6 to v_6 , i.e., rainfall in June affecting the June NDVI values). A circle at the end of an edge indicates that there exists a relationship between variables connected by the edge (e.g., v_4 to r_7 or April NDVI and July rainfall), but the data are not sufficient for the algorithm to determine the direction of the relationship.

[44] Figure 13a displays the results obtained from CCD algorithm. From Figure 13a, it is evident that v_3 , v_4 , and v_5 are related. Further v_4 is connected to r_7 . Because the different structures indicate different months a direction can be intuitively interpreted. For example, the April NDVI

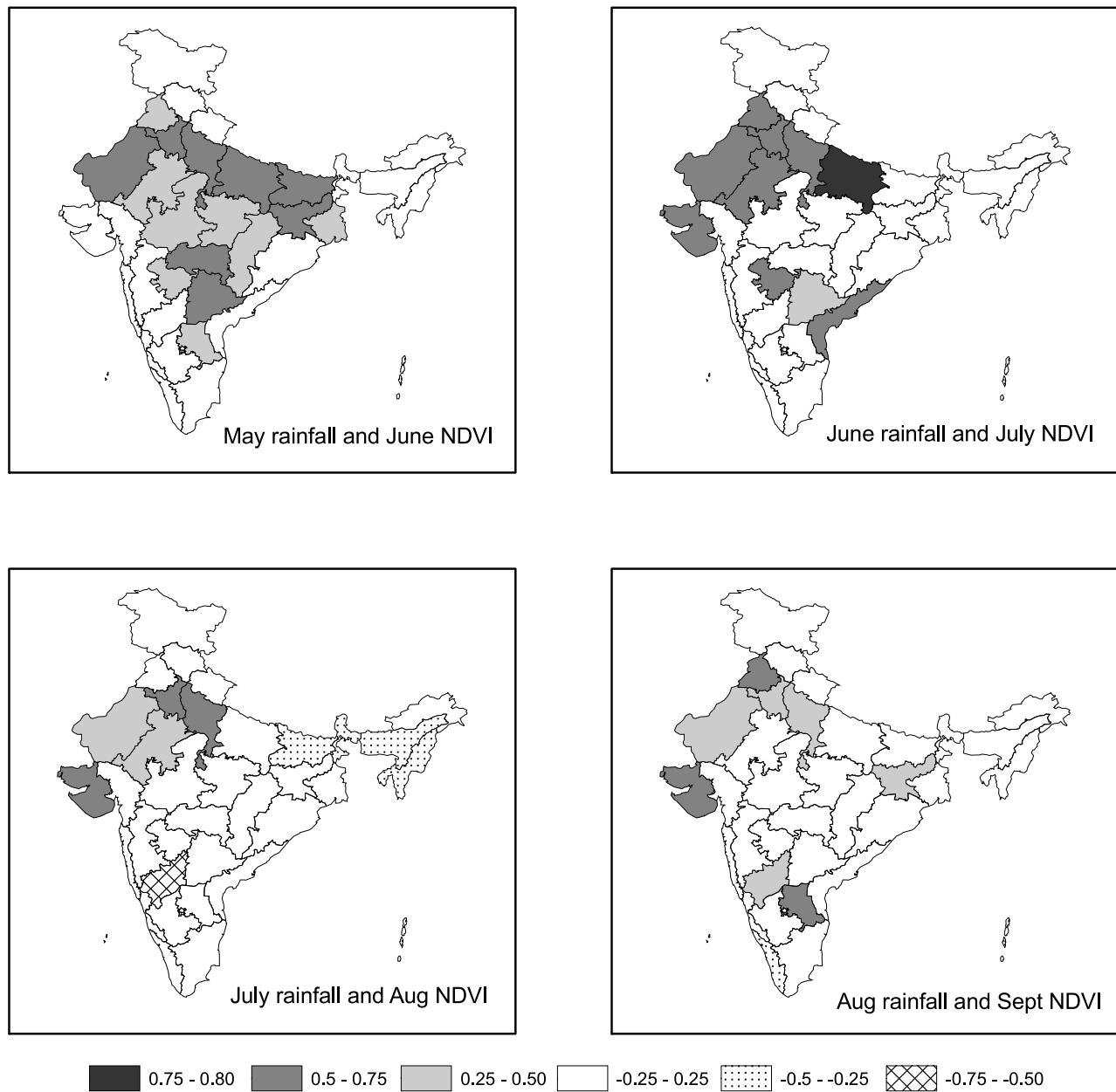


Figure 12. One month lag correlation between NDVI values and rainfall during monsoon months (June–July–August). Subdivisions with correlation significant at 10% level are shaded.

(v4) would be related to March NDVI (v3) rather than the other way round.

[45] The acyclic analysis from the LiNGAM algorithm (Figure 13b) shows that NDVI value of March (v3) affects April NDVI (v4) which in turn affects May NDVI (v5) and July rainfall (r7). The relationships between NDVIs are positive whereas that between April NDVI and July rainfall is negative. The data do not reveal any relationship that involves June NDVI and June rainfall. However, there exist additional information regarding relationships between v5, v6, and r6 in CCD results that was not present in LiNGAM output. Note that both algorithms can only discover linear causal relations. Further, the CCD algorithm does not provide the strength or nature (\pm sign) of the causal relationship if there is confounding. We note that both the algorithms did not find any causal relationship between

NDVI and rainfall over other groups of subdivisions, corroborating the results from correlation analysis.

[46] To test the presence of causal relationship between NDVI and rainfall during monsoon months, causal algorithm was applied to all the subdivisions grouped together. The existence of such cause-effect relationship was suggested by correlation analysis (Figures 11 and 12). Figure 14 presents the results from the LiNGAM and CCD analysis. The results obtained from both the algorithms share some common features. For example, June rainfall (r6) and June NDVI (v6) affects July NDVI (v7). Further, June and July NDVI have some bearing on August NDVI (v8). CCD result indicates that July rainfall (r7) influences July NDVI (v7), whereas such a link is not present in LiNGAM output. So, both the approaches together, provide a more complete

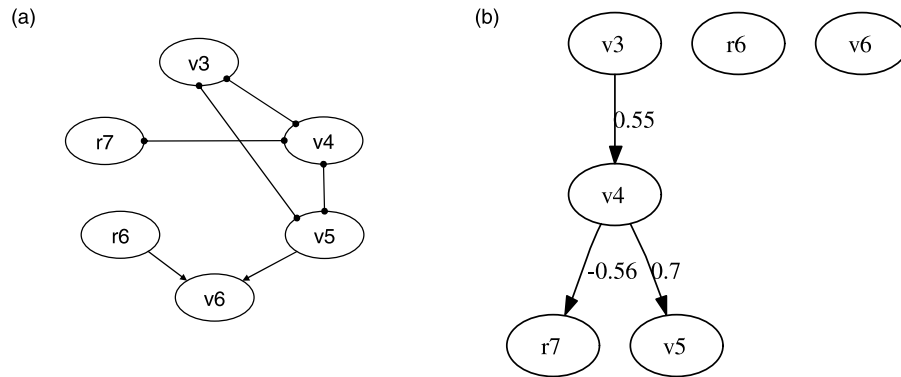


Figure 13. (a) Causal structure obtained from cyclic causal discovery (CCD) algorithm. (b) Directed acyclic graph from LiNGAM algorithm. Letter “v” denotes NDVI and “r” denotes rainfall. The index associated with a letter represents month. The results correspond to meteorological subdivisions in southern India.

picture of the potential feedback between land use changes and Indian summer monsoon rainfall change.

[47] To understand the physical mechanism regarding the impact of premonsoon land surface processes and vegetation on the monsoon circulation (and hence rainfall), we analyzed the premonsoon area-aggregated NDVI variation and monsoon boundary layer and upper air convergence patterns over India (Figure 15a). When analyzing the energetics of the Indian monsoon system, *Krishnamurti et al.* [1998] concluded that radiative heating is the biggest contributor to the overall generation of available potential energy (APE) for the monsoon system. The other components of the heating that contribute to the generation of APE are radiative flux convergence and the sensible heat fluxes from land and ocean surface. *Krishnamurti et al.* [1998] showed that the conversion of APE to the kinetic energy can be understood in terms of the covariances between (1) heating and temperature, (2) temperature and vertical velocity (associated with thermal circulation) leading to the conversion of APE to kinetic energy of divergent motion, and (3) gradients of stream function and velocity potential resulting in the conversion of divergent kinetic energy to rotational

kinetic energy. Thermal circulation can be manifested as a converging and upward motion at surface boundary layer along with a compensating divergent circulation at upper tropospheric levels. The largest contribution of these conversions are generally found at 200–300 hPa level as the monsoon warm core resides near these levels. The areas of divergent circulation and magnitude of vertical velocities are also large at these levels, and small changes in these fields due to alteration of the components of energy exchange processes can be detected at these levels.

[48] Consistent with the changing patterns of agriculture over the Indian region, the premonsoon NDVI shows a significant increasing trend. We selected the years 1989 and 1998, respectively, to denote the years with lowest and highest premonsoon NDVI over India. Figure 15b shows the difference of 200 mbar wind divergence between 1998 and 1989 for the month of July. A large-scale negative divergence (convergence) anomaly that covers entire southern India and the monsoon trough region over the north India can be noted. Interestingly, the only region that shows the positive divergence anomaly is the western part of India which has a strong topographical influence due to the

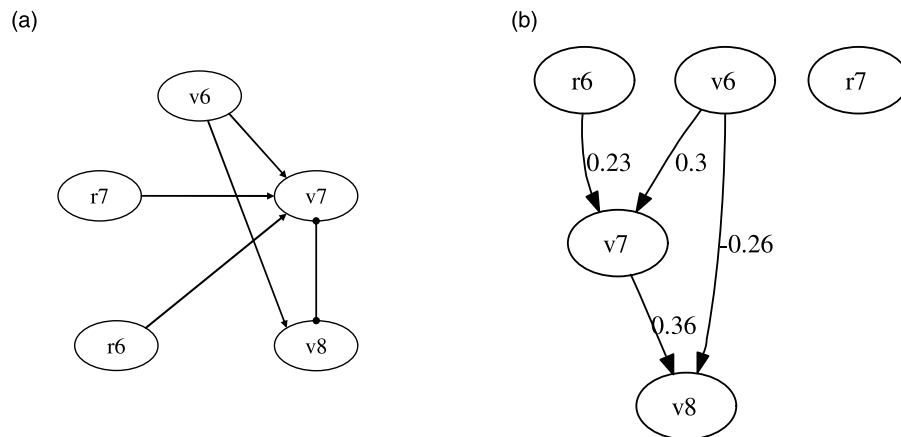


Figure 14. (a) Causal structure obtained from CCD algorithm. (b) Directed acyclic graph from LiNGAM algorithm. Letter “v” denotes NDVI and “r” denotes rainfall. The index associated with a letter represents month. The results are based on the data from all the meteorological subdivisions of India.

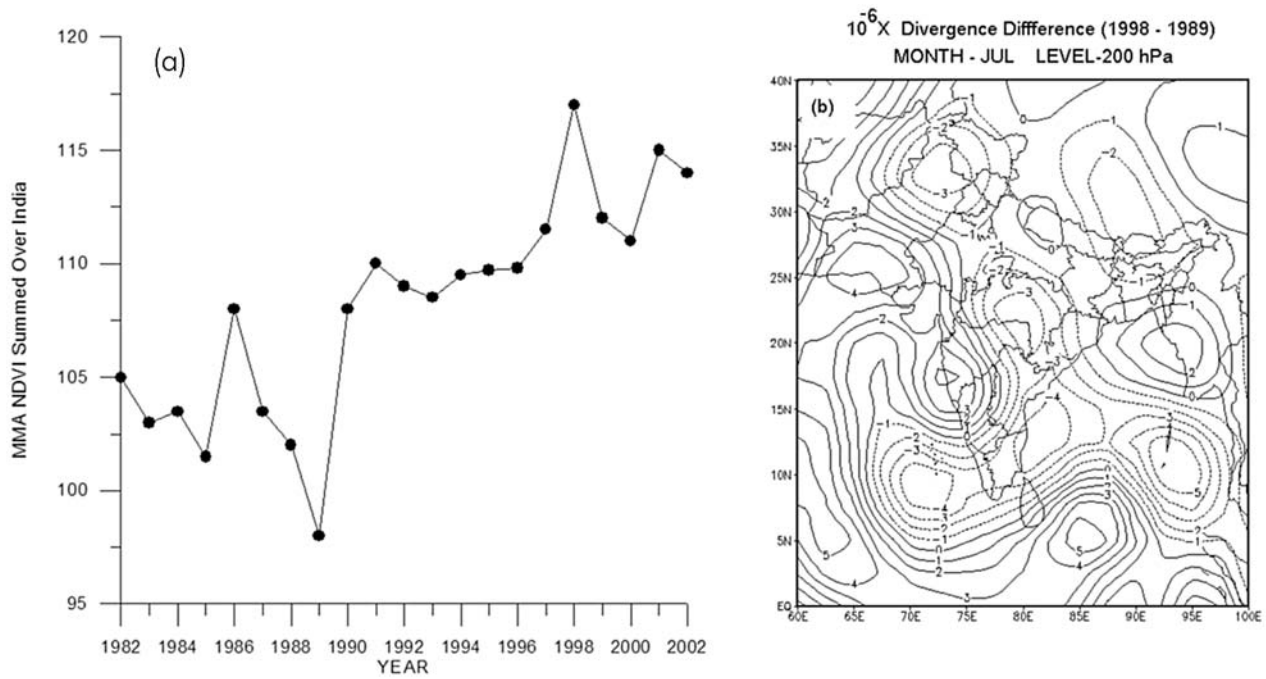


Figure 15. (a) Area-aggregated NDVI during the months of March–April–May. (b) The 200 mbar wind divergence between 1998 (lowest NDVI) and 1989 (highest NDVI) for the month of July.

Western Ghats. A consistent pattern was seen in the 850 mbar plots with a convergence zone over the NW India region (figure not shown). The negative divergence anomalies at upper level represent a weakened monsoon circulation that can be attributed to a weaker wind convergence at the lower levels. *Lee et al.* [2008] also reported a similar relationship between large-scale vegetation during spring season, and the upper level circulation during July, over the southwest monsoon region. Thus, building on the results of the causal discovery algorithm, the dynamical analysis further affirms that the increased vegetation during the premonsoon season negatively affects the monsoon circulation, and hence, the monsoon rainfall.

6. Conclusions

[49] Observational analysis of the rainfall and land use data set over the Indian monsoon region provides insights into the potential role of agricultural intensification and land use changes in affecting the Indian summer monsoon.

[50] Observations based on satellite remote sensing can help in explaining the physical mechanism behind the long-term regional trends in Indian summer monsoon rainfall. One such region is the north/northwest India, which shows a significant decline of rainfall in past few decades and was detected by both EOF- and GA-based analyses. Our analysis provides growing evidence that the change in rainfall climatology in north/northwest India is caused by anthropogenic land use modifications due to agricultural intensification.

[51] The NDVI data showed that over past two decades, January–February–March vegetation index has increased mainly over agricultural (wheat producing) regions in India. The soil moisture data show a significant increase over the agricultural region and seem to cause significant decrease in the subsequent rainfall. However, for April and May

(months just before start of monsoon season), the vegetation index has increased only over Peninsular India.

[52] The correlation analysis and causal discovery algorithms suggested that April month vegetation index has some bearing on July month precipitation over peninsular India. In particular, there exists a negative relationship between them. However, exact quantification of the relationship was not feasible due to the limited record length.

[53] The causal discovery algorithms presented in the study have a promising feature of discovering cause-effect relationships from observed climatic data sets. However, the algorithms are still in their infancy and assume linear cause-effect relationships. Further, these algorithms assume that there are no unobserved confounders, an assumption that is seldom true of environmental observations. Thus, caution should be exercised in interpreting results from causal discovery algorithms and should be used in conjunction with physically consistent process scale studies. It was also beyond the scope of this study to compare the role of land surface versus sea surface temperature changes that have well-known significant impact on monsoon rainfall (e.g., *Rasmusson and Carpenter* [1983]; however, also see *Kumar et al.* [1999]).

[54] Further, the cause and effect relation needs to be interpreted cautiously. A lower rainfall can reduce vegetation (NDVI) and this in turn, our analysis indicates, lead to increased potential for rainfall anomaly. The threshold for what constitutes an organized land use land cover change to impact the rainfall patterns remains to be identified. Preliminary analysis from an ongoing study suggest and our current observational results, complemented by other recent findings reported by *Douglas et al.* [2006, 2009], and *Lee et al.* [2008] provide strong evidence that the land surface feedback due to agricultural intensification/irrigation over northern India has become sufficiently coherent or orga-

nized to impact the regional rainfall processes. This leads to the conclusion that the rainfall variability over the Indian monsoon region is modulated by the antecedent land surface conditions; and that the longer-term rainfall reduction is linked to the agricultural intensification and irrigation. It will be interesting to assess whether the feedback identified in this study is unique for the Indian monsoon region or whether it can be seen in other monsoon regions across the globe. It is likely that high land-atmosphere coupling areas of India, Sahel, and possibly U.S. Great Plains [Douville *et al.*, 2001; Koster *et al.*, 2004] may show this signature. However, the high moisture flux and the intensity of agricultural change noted over India would potentially make it a dominant signal as compared to other regions such as over Sudan-Sahel and southwest American monsoon domains [Niyogi *et al.*, 2002b].

[55] The results of this study, while not unconditional, do suggest that unsustainable, increase in agricultural intensification could reduce the monsoon rainfall over India. The results are more robust over northern and Peninsular India, indicating that increase in NDVI may have been partly responsible for weakening the early monsoon rainfall in this region. The impact of future land use changes would need to be considered in providing more robust constraints for future climate change simulations over the Indian monsoon region.

[56] **Acknowledgments.** Study benefited in from the NSF CAREER ATM (Liming Zhou and Jay Fein), and also benefited from NASA-THP (Jared Entin NNG05GQ47G and NNG06GH17G), NASA LCLUC Program (G. Gutman). We thank Ellen Douglas at University of Massachusetts at Boston for her comments on the draft version of this manuscript. We also thank useful suggestions from the Editor (S. Tyler), and anonymous comments from the associate editor, and from the three reviewers which helped clarify the presentation. In particular, we thank one of the reviewers for providing us with the NDVI rainfall study by Lee *et al.* (unpublished manuscript, 2009).

References

- Adler, R. F., *et al.* (2003), The version-2 global precipitation climatology project (GPCP) monthly precipitation analysis (1979–present), *J. Hydrometeorol.*, **4**, 1147–1167, doi:10.1175/1525-7541(2003)004<1147:TVGPCP>2.0.CO;2.
- Basist, A., N. Grody, T. Peterson, and C. Williams (1998), Using Special Sensor Microwave Imager to monitor land surface temperature, soil wetness, and snow cover, *J. Appl. Meteorol.*, **37**, 888–911, doi:10.1175/1520-0450(1998)037<0888:UTSSMI>2.0.CO;2.
- Bonan, G. B. (2002), *Ecological Climatology: Concepts and Applications*, 678 pp., Cambridge Univ. Press, Cambridge, U. K.
- Chang, H., D. Niyogi, A. Kumar, C. Kishtawal, J. Dudhia, F. Chen, U. C. Mohanty, and M. Sheperd (2009), Possible relation between land surface feedback and the post-landfall structure of monsoon depression, *Geophys. Res. Lett.*, **36**, L15826, doi:10.1029/2009GL037781.
- Douglas, E., D. Niyogi, S. Frolking, J. B. Yeluripati, R. A. Pielke Sr., N. Niyogi, C. J. Vörösmarty, and U. C. Mohanty (2006), Changes in moisture and energy fluxes due to agricultural land use and irrigation in the Indian Monsoon belt, *Geophys. Res. Lett.*, **33**, L14403, doi:10.1029/2006GL026550.
- Douglas, E. M., A. Beltrán-Przekurat, D. Niyogi, R. A. Pielke Sr., and C. J. Vörösmarty (2009), The impact of agricultural intensification and irrigation on land-atmosphere interactions and Indian monsoon precipitation: A mesoscale modeling perspective, *Global Planet. Change*, **67**, 117–128, doi:10.1016/j.gloplacha.2008.12.007.
- Douville, H., E. Chauvin, and H. Broqua (2001), Influence of soil moisture on the Asian and African monsoons. Part I: Mean monsoon and daily precipitation, *J. Clim.*, **14**, 2381–2403, doi:10.1175/1520-0442(2001)014<2381:IOSMOT>2.0.CO;2.
- Feddema, J. J., K. W. Oleson, G. B. Bonan, L. O. Mearns, L. E. Buja, G. A. Meehl, and W. M. Washington (2005), The importance of land-cover change in simulating future climates, *Science*, **310**, 1674–1678, doi:10.1126/science.1118160.
- Fein, J. S., and P. L. Stephens (1987), *Monsoons*, 654 pp., Wiley-Interscience, Washington, D. C.
- Foley, J., *et al.* (2005), Global consequences of land use, *Science*, **309**, 570–574, doi:10.1126/science.1111772.
- Fu, C. (2003), Potential impacts of human-induced land cover change on East Asia monsoon, *Global Planet. Change*, **37**, 219–229.
- Goldman, A., and J. Smith (1995), Agricultural transformations in India and northern Nigeria: Exploring the nature of green revolutions, *World Dev.*, **23**, 243–263, doi:10.1016/0305-750X(94)00115-F.
- Goswami, B. N. (2004), South Asian summer monsoon: An overview, in *The Global Monsoon System: Research and Forecast*, edited by C. P. Chang, B. Wang, and N. C. G. Lau, *Tech. Doc. WMO-TD 1266*, pp. 47–71, World Meteorol. Org., Geneva.
- Goswami, B. N., V. Venugopal, D. Sengupta, M. S. Madhusoodanan, and P. K. Xavier (2006), Increasing trend of extreme rain events over India in a warming environment, *Science*, **314**, 1442–1445, doi:10.1126/science.1132027.
- Houze, R. A., Jr., D. C. Wilton, and B. F. Smull (2007), Monsoon convection in the Himalayan region as seen by the TRMM precipitation radar, *Q. J. R. Meteorol. Soc.*, **133**, 1389–1411, doi:10.1002/qj.106.
- Hume, D. (1999), *An Enquiry Concerning Human Understanding: A Critical Edition*, edited by T. L. Beauchamp, Oxford Univ. Press, New York.
- Intergovernmental Panel on Climate Change (IPCC) (2007), *Climate Change 2007: The Physical Science Basis, Contribution of Working Group I to the Fourth Assessment Report of the Intergovernmental Panel on Climate Change*, edited by S. Solomon *et al.*, Cambridge Univ. Press, Cambridge, U. K.
- Jeyaseelan, A. T., P. S. Roy, and S. S. Young (2007), Persistent changes in NDVI between 1982 and 2003 over India using AVHRR GIMMS (Global Inventory Modeling and Mapping Studies) data, *Int. J. Remote Sens.*, **28**, 4927–4946, doi:10.1080/01431160701253279.
- Joshi, P. K., and N. K. Tyagi (1991), Sustainability of existing farming systems in Punjab and Haryana: Some issues in ground water used, *Indian J. Agric. Econ.*, **46**, 412–421.
- Kishtawal, C. M., P. K. Pal, and M. S. Narayanan (1991), Water vapor periodicities over Indian Ocean during contrasting monsoons from NOAA satellite data, *Proc. Indian Acad. Sci.*, **100**, 341–359.
- Kishtawal, C. M., S. Basu, F. Patadia, and P. K. Thapliyal (2003), Forecasting summer rainfall over India using genetic algorithm, *Geophys. Res. Lett.*, **30**(23), 2203, doi:10.1029/2003GL018504.
- Kishtawal, C. M., D. Niyogi, M. Tewari, R. A. Pielke Sr., and M. Shepherd (2010), Urbanization signature in the observed heavy rainfall climatology over India, *Int. J. Climat.*, in press.
- Koster, R. D., *et al.* (2004), Regions of strong coupling between soil moisture and precipitation, *Science*, **305**, 1138–1140, doi:10.1126/science.1100217.
- Krishnamurti, T. N., M. C. Sinha, B. Jha, and U. C. Mohanty (1998), A study of south Asian monsoon energetic, *J. Atmos. Sci.*, **35**, 2530–2548, doi:10.1175/1520-0469(1998)055<2530:ASOSAM>2.0.CO;2.
- Krishnamurti, T. N., C. M. Kishtawal, T. E. LaRow, D. R. Bachiochi, Z. Zhang, C. E. Williford, S. Gadgil, and S. Surendran (1999), Improved weather and seasonal climate forecasts from multimodel superensemble, *Science*, **285**, 1548, doi:10.1126/science.285.5433.1548.
- Kumar, K., B. Rajagopalan, and M. A. Cane (1999), On the weakening relationship between the Indian monsoon and ENSO, *Science*, **284**, 2156–2159, doi:10.1126/science.284.5423.2156.
- Lee, E., T. N. Chase, B. Rajagopalan, R. G. Barry, T. W. Biggs, and P. J. Lawrence (2008), Effects of irrigation and vegetation activity on early Indian summer monsoon variability, *Int. J. Climatol.*, **29**, 573–581, doi:10.1002/joc.1721.
- Medina, S., R. A. Houze Jr., A. Kumar, and D. Niyogi (2010), Summer monsoon convection in the Himalayan region: Terrain and land cover effects, *Q. J. R. Meteorol.*, in press.
- Meehl, G. A., and W. M. Washington (1993), South Asian summer monsoon variability in a model with doubled atmospheric carbon dioxide concentration, *Science*, **260**, 1101–1104, doi:10.1126/science.260.5111.1101.
- Mitchell, M. (1998), *An Introduction to Genetic Algorithms*, 221 pp., MIT Press, Boston, Mass.
- Mooley, D. A., and B. Parthasarathy (1984), Fluctuations of all-india summer monsoon rainfall during 1871–1978, *Clim. Change*, **6**, 287–301.
- Niyogi, D., Y. Xue, and S. Raman (2002a), Hydrological land surface response in a tropical regime and a midlatitudinal regime, *J. Hydrometeorol.*, **3**, 39–56, doi:10.1175/1525-7541(2002)003<0039:HLSRIA>2.0.CO;2.

- Niyogi, D., R. A. Pielke Sr., K. Alapaty, J. Eastman, T. Holt, U. C. Mohanty, S. Raman, T. K. Roy, and Y. K. Xue (2002b), Challenges of representing land surface processes in weather and climate models over Tropics: Examples over the Indian subcontinent, in *Weather and Climate Modeling*, edited by S. V. Singh, S. Basu, and T. N. Krishnamurti, pp. 132–145, New Age Int., New Delhi.
- Niyogi, D., H. Chang, F. Chen, L. Gu, A. Kumar, S. Menon, and R. A. Pielke Sr. (2007), Potential impacts of aerosol-land-atmosphere interaction on the Indian monsoonal rainfall characteristics, *Nat. Hazards*, *42*, 345–359, doi:10.1007/s11069-006-9085-y.
- O'Brien, K., et al. (2004), Mapping vulnerability to multiple stressors: Climate change and globalization in India, *Global Environ. Change*, *14*, 303–313, doi:10.1016/j.gloenvcha.2004.01.001.
- Parthasarathy, B., K. Rupa Kumar, and A. A. Munot (1991), Evidence of secular variations in Indian summer monsoon rainfall-circulation relationships, *J. Clim.*, *4*, 927–938, doi:10.1175/1520-0442(1991)004<0927:EQSVII>2.0.CO;2.
- Parthasarathy, B., A. A. Munot, and D. R. Kothawale (1994), All India monthly and seasonal rainfall series: 1871–1993, *Theor. Appl. Climatol.*, *49*, 217–224, doi:10.1007/BF00867461.
- Pearl, J. (2000), *Causality: Models of Reasoning and Inference*, Cambridge Univ. Press, Cambridge, U. K.
- Peixoto, J. P., and A. H. Oort (1992), *Physics of Climate*, 564 pp., Am. Inst. of Phys., New York.
- Pielke, R. A., Sr., G. Marland, R. A. Betts, T. N. Chase, J. L. Eastman, J. O. Niles, D. Niyogi, and S. Running (2002), The influence of land-use change and landscape dynamics on the climate system: Relevance to climate change policy beyond the radiative effect of greenhouse gases, *Philos. Trans. R. Soc. London, Ser. A*, *360*(special issue), 1705–1719.
- Pielke, R. A., Sr., D. S. Niyogi, T. N. Chase, and J. Eastman (2003), A new perspective on climate change and variability: A focus on India, Invited paper to the Advanced in Atmospheric and Oceanic Sciences, *Proc. Indian Natl. Sci. Acad.*, *69*, 107–123.
- Pielke, R. A., Sr., J. Adegoke, A. Beltran-Przekurat, C. A. Hiemstra, J. Lin, U. S. Nair, D. Niyogi, and T. E. Nobis (2007), An overview of regional land use and land cover impacts on rainfall, *Tellus, Ser. B*, *59*, 587–601, doi:10.1111/j.1600-0889.2007.00251.x.
- Rajeevan, M., J. Bhate, J. D. Kale, and B. Lal (2006), High resolution daily gridded rainfall data for Indian region: Analysis of break and active monsoon spells, *Curr. Sci.*, *91*, 296–306.
- Ramanathan, V., P. J. Crutzen, J. T. Kiehl, and D. Rosenfeld (2001), Aerosols, climate, and the hydrological cycle, *Science*, *294*, 2119–2124, doi:10.1126/science.1064034.
- Ramanathan, V., C. Chung, D. Kim, T. Bettge, L. Buja, J. T. Kiehl, W. M. Washington, Q. Fu, D. R. Sikka, and M. Wild (2005), Atmospheric brown clouds: Impacts on South Asian climate and hydrological cycle, *Proc. Natl. Acad. Sci. U. S. A.*, *102*, 5326–5333, doi:10.1073/pnas.0500656102.
- Rasmusson, E. M., and T. H. Carpenter (1983), The relationship between eastern equatorial pacific sea surface temperatures and rainfall over India and Sri Lanka, *Mon. Weather Rev.*, *111*, 517–528, doi:10.1175/1520-0493(1983)111<0517:TRBEEP>2.0.CO;2.
- Richardson, T. (1996), A discovery algorithm for directed cyclic graphs, in *Proceedings of the 12th Conference on Uncertainty in Artificial Intelligence*, edited by E. Horvitz and F. Jensen, pp. 456–460, Morgan Kaufmann, San Francisco, Calif.
- Roy, S. S., R. Mahmood, D. Niyogi, M. Lei, S. A. Foster, K. G. Hubbard, E. Douglas, and R. Pielke Sr. (2007), Impacts of the agricultural green revolution-induced land use changes on air temperatures in India, *J. Geophys. Res.*, *112*, D21108, doi:10.1029/2007JD008834.
- Shepard, D. (1968), A two-dimensional interpolation function for irregularly spaced data, ACM, in *Proceedings of the 23rd ACM National Conference*, pp. 517–524, Assoc. for Comput. Mach., New York.
- Shimizu, S., P. O. Hoyer, A. Hyvärinen, and A. J. Kerminen (2006), A linear non-Gaussian acyclic model for causal discovery, *J. Mach. Learn. Res.*, *7*, 2003–2030.
- Sikka, D. R., and S. Gadgil (1980), On the maximum cloud zone and the ITCZ over Indian longitude during southwest monsoon, *Mon. Weather Rev.*, *108*, 1840–1853, doi:10.1175/1520-0493(1980)108<1840:OTMCZA>2.0.CO;2.
- Singh, R. P., S. R. Oza, and M. R. Pandya (2006), Observing long-term changes in rice phenology using NOAA–AVHRR and DMSP–SSM/I satellite sensor measurements in Punjab, India, *Curr. Sci.*, *91*, 1217–1221.
- Sinha Ray, K. C., and S. Srivastava (2000), Is there any change in extreme events like heavy rainfall?, *Curr. Sci.*, *79*, 155–158.
- Spirtes, P., C. Glymour, and R. Scheines (1993), *Causation, Prediction, and Search*, Springer, New York.
- Srivastava, H. N., B. N. Dewan, S. K. Dikshit, G. S. Prakash Rao, S. S. Singh, and K. R. Rao (1992), Decadal trends in Climate over India, *Mausam*, *43*, 7–20.
- Tucker, C. J., J. E. Pinzon, M. E. Brown, D. A. Slayback, E. W. Pak, R. Mahoney, E. F. Vermote, and N. El Saleous (2005), An extended AVHRR 8-km NDVI data Set compatible with MODIS and SPOT vegetation NDVI Data, *Int. J. Remote Sens.*, *26*, 4485–4498, doi:10.1080/01431160500168686.
- Webster, P. J., V. O. Magana, T. N. Palmer, J. Shukla, R. T. Tomas, M. Yanai, and T. Yasunari (1998), Monsoons: Processes, predictability and the prospects of prediction, *J. Geophys. Res.*, *103*(C7), 14,451–14,510, doi:10.1029/97JC02719.
- Yasunari, T. (1979), Cloudiness fluctuations with the northern hemisphere summer monsoon, *J. Meteorol. Soc. Jpn.*, *57*, 227–242.

R. S. Govindaraju and S. Tripathi, School of Civil Engineering, Purdue University, Stadium Mall, West Lafayette, IN 47907, USA.

C. Kishtawal, Space Applications Center, Indian Space Research Organization, Ahmadabad 380015, India.

D. Niyogi, Department of Agronomy, Purdue University, Lilly Hall of Sciences, West Lafayette, IN 47906-2054, USA. (dniyogi@purdue.edu)